Periodic Small-Signal Analysis as a Tool to Build Transient Stability Models of VSC-based Devices

F. Bizzarri, A. Brambilla, S. Grillo
DEIB, Politecnico di Milano,
p.za Leonardo da Vinci, 32,
I-20133, Milano, Italy
{federico.bizzarri,angelo.brambilla,samuele.grillo}@polimi.it

F. Milano
School of Electrical and Electronic Engineering,
University College Dublin,
Belfield, Dublin 4, Ireland
federico.milano@ucd.ie

***Abstract*—The paper introduces a novel approach to derive a dynamic model of devices with inclusion of Voltage Source Converter (VSC) devices suitable for transient angle and voltage stability analysis of power systems. With this aim, we treat the VSC as a nonlinear switched set of equations and apply a time-domain shooting method to define the behaviour of such model at the fundamental frequency of the system. Then the time-varying small-signal model of the VSC is derived through periodic small-signal analysis. The resulting model is defined in terms of a transfer function from which we can define a lumped equivalent circuit of the original device. The proposed approach is discussed and tested through the study of the transient response of a Static VAR Compensator (STATCOM) device connected to the well-known IEEE 14-bus system.**

***Index Terms*—Harmonic analysis, analog/mixed signal analysis, small signal periodic analysis, voltage source converter.**

I. Introduction

A. Motivation

In recent years, Voltage Source Converter (VSC)-based converters have become omnipresent in power system applications. Second generation Flexible AC Transmission System (FACTS) devices, wind power plants (based on double-fed induction generators and systems with full-scale back-to-back converters [1], [2]) and solar photovoltaic power plants are all based on VSC converters. With this aim, comprehensive overviews of the solutions based on power-electronics for distributed generation can be found in [3], [4]. Other relevant medium voltage applications range from the control of large induction and synchronous motors [5] to pumped storage energy systems [6]. This paper deals with an accurate representation of the interaction of power system models and highly non linear power electronics circuits.

B. Literature Review

The conventional model of the VSC used in power system studies is an approximated balanced, fundamental frequency model, as proposed in [7]–[12]. This model includes dc circuit and phase-locked loop dynamics as well as an average dq-axis model of the converter and an equivalent model for switching losses. In this paper we proceed using a completely different approach. Instead of defining an average dq-axis model of the converter, we start our analysis using the fully-fledged three-phase nonlinear switched model of the VSC. Then, we study its response at the fundamental frequency and define an equivalent circuit resembling such a response (see next subsection for further details).

Pioneering works based on this approach find their roots in the Harmonic Power Flow (HPF) analysis [13], [14]. Recent studies have focuses on dynamic phasor modelling that preserve a given approximated harmonic content of the original nonlinear system [15]. Both the HPF and dynamic phasor modelling approaches are actually specialised versions of solving the nonlinear power system in the frequency domain and finds the "full" spectrum on the solution. This approach is actually a specialised version of the more general Harmonic Balance (HB) method [16], which is largely used in electronic engineering and circuit theory applications. The HB method is particularly suited to determine the steady-state solution of mildly nonlinear circuits in the frequency domain. However, one of the main issues affecting the HB and, hence, the HPF is that some nonlinear models, such as the VSC, can not be modelled in the frequency domain.

A different approach presented in the literature is to build an extended admittance model of the nonlinear load working at steady-state that links the load current to the applied voltage by taking into account also intermodulation effects [17]. This means that a perturbation of the feeder current, described by an envelope is mapped as a current at the same frequency (of the envelope) and as beats located at frequencies that are multiple of the converter working frequency (harmonics).

C. Proposed Technique and Contribution

In this paper, we propose a technique to characterize the frequency response of nonlinear switched devices such as the VSC. The main steps of the proposed technique are as follows.

- Compute the steady-state solution of the nonlinear switching load (power converter). This is performed in the time domain through an enhanced version of the shooting method able to deal with hybrid dynamic systems [18], [19].
- Perform a Periodic Small Signal (PAC) analysis by injecting a small signal perturbation in peculiar nodes of the circuit. Effects of the small signal are assumed additive and does not substantially alters the main orbit of the switching load [20].

- Build a frequency domain model, i.e., a "generalised" Norton equivalent (based on an intermodulation admittance matrix and equivalent sources) that allows capturing the rich spectrum of the nonlinear load. This model can be synthesised, for example, by exploiting rational polynomials as it is done to build lumped model of distributed elements such as waveguides [21].

The resulting equivalent model can be used for angle and voltage stability analysis of power systems. The approach introduced above is applied to characterise a three-phase VSC that works driven by a PWM waveform at 9 f_o (where f_o is the overall working frequency) with an analog/digital controller that sets the i_d active and i_q reactive currents from a three-phase voltage source. As an example, we apply the VSC model described above to a Static VAR Compensator (STATCOM), which is a shunt FACTS device used to control the voltage amplitude at the point of connection. The proposed equivalent single-phase model of the STATCOM is finally thoroughly tested through a case study based on IEEE 14-BUS test system.

II. Background Elements

A. Power System Modeling Approach

General power system models are formulated so that their equilibrium points (viz. power flow solutions) represent the (constant) envelope of the corresponding time domain waveforms at the reference working frequency, hence adopting a phasorial representation of the system variables. However, such an approach implicitly neglects the potentially rich harmonic content of nonlinear devices, such as those based on power electronic converters.

For the sake of discussion, we express the harmonic content through the Fourier series representation of a generic time domain solution of the power system viewed as a fully-dynamic system. Consider the periodic function:

$$x(t) = c_0 + \sum_{k=1}^{\infty} c_k \cos(2\pi k f_o t + \phi_k) \quad , \tag{1}$$

where $f_o \in \mathbb{R}^+$ is the fundamental frequency and c_0, c_k and ϕ_k are real. If we rewrite (1) by putting in evidence the first harmonic of the periodic solution

$$x(t) = \mathrm{Re}\left\{ \overbrace{c_1 e^{\mathrm{i}\phi_1}}^{x_{PF}} e^{\mathrm{i}2\pi f_o t} \right\} + \overbrace{c_0 + \sum_{k=2}^{\infty} c_k \cos(2\pi k f_o t + \phi_k)}^{\Psi(t)} \quad , \tag{2}$$

we have that x_{PF} is the phasor computed by the power flow analysis and $\Psi(t)$ represents the discarded harmonic content. This basically means that the effects of $\Psi(t)$ are assumed to be not relevant and the power system (at steady state) behaves in a purely sinusoidal steady-state. In Fig. 1, it is shown the Power Spectral Density (PSD) of $x(t)$ together with other information; blue impulses represent neglected harmonics whereas red ones are the fundamental components at $\pm f_o$. Obviously the more the PSD of $\Psi(t)$ is lower than $c_1^2/2$ the more the phasorial assumption is valid.

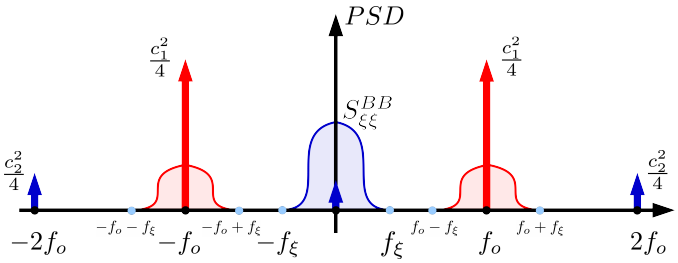

Figure 1. Sketch of the PSD of the generic variable $x(t)$ in Eq. (2) (red and blue pulses) and of the envelope modulation $\xi(t)$ (blue area) centered at f_o and then shifted in baseband (gray area). Only the first two harmonics of the spectrum of $x(t)$ are represented, although, in principle, the spectrum is infinite.

Despite the aforementioned phasorial approach, the model of the power system is conceived in a mixed way. Some elements, e.g., transmission lines and transformers, are described by linear algebraic equations in complex algebra, whereas some others, such as for example generators, are described by Differential Algebraic Equations (DAEs). These DAEs lead to time varying solutions representing modulations of the sinusoidal waveform corresponding to x_{PF}, i.e., c_1 and ϕ_1 are functions of time. The power system model thus provides a small signal $\xi(t)$ to be "superimposed" to $\mathrm{Re}\left\{x_{PF} e^{\mathrm{i}2\pi f_o t}\right\}$. Although the spectrum of $\xi(t)$ is actually centered at f_o (see the red areas in Fig. 1), the power system model operates a frequency shift and provides a baseband version of this signal (see the $S_{\xi\xi}^{BB}$ blue area in Fig. 1).[1]

B. On the Periodic Small Signal Analysis

The above summarized power system representation is quite similar to what is done when dealing with nonlinear circuits operating at periodic steady state, if we are interested in analysing, through Periodic Small Signal (PAC) analysis, the effect of small signal perturbations. Consider the following index-1 DAE describing the dynamics of a periodically forced circuit (with period $T = 1/f_o$)

$$\frac{d}{dt} q(t, y) + j(t, y) = 0 \quad , \tag{3}$$

where $0 \in \mathbb{R}^N$. If the circuit admits a periodic steady state behaviour then $y_s(t) = y_s(t + T) \in \mathbb{R}^N$ is a solution of (3). We are interested in studying how a small additive perturbation $\eta(t) \in \mathbb{R}^N$, acting as

$$\frac{d}{dt} q(t, y) + j(t, y) + \eta(t) = 0 \quad , \tag{4}$$

[1] It is worth recalling that this formulation is valid if the spectrum of $\xi(t)$ is bounded and its maximum significant frequency is lower than f_o [22]. Nevertheless, this hypothesis is usually not verified and this modeling approach is adopted to simulate fast transient phenomena. A relevant case is, for example, whenever one of the power system variables exhibits a discontinuity during its transient evolution that actually implies an infinite frequency spectrum of that variable.

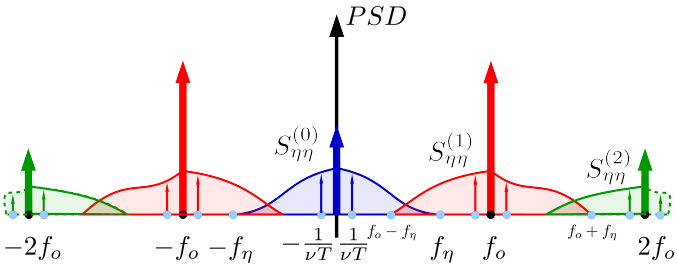

Figure 2. Sketch of both the impulsive PSD of one of the components of the $y_s(t)$ periodic steady state solution of (3) and the PSD of the same component of $y_\eta(t)$ that is obtained by summing the $S^{(k)}_{\eta\eta}$ contributions ($k \geq 0$).

affects $y_s(t)$. With this aim, (3) can be linearized along its periodic orbit thus leading to

$$\frac{d}{dt}\left(\underbrace{\left.\frac{\partial q(t,y)}{\partial y}\right|_{y=y_s}}_{C(t)} y_\eta\right) + \left(\underbrace{\left.\frac{\partial j(t,y)}{\partial y}\right|_{y=y_s}}_{G(t)} y_\eta\right) + \eta(t) = 0 \quad , \tag{5}$$

and it is assumed that the solution of the original non linear circuit can be written as $y(t) = y_s(t) + y_\eta(t)$. Matrices $C(t)$ and $G(t)$ are characterized by T-periodic entries and (5) is a Linear Time-Varying Periodic DAE. If $\eta(t)$ is a purely sinusoidal vector with period νT ($\nu \in \mathbb{R}$), the spectrum of the y_η solution contains frequencies of the form $\pm 1/\nu T + k f_o$ ($k \in \mathbb{Z}$), i.e., frequency folding occurs [23]. This is exemplified in Fig. 2 where the harmonics at kf_o refer to the large signal solution. In general, if the spectrum of $\eta(t)$ is richer than a single tone and confined in the frequency interval $[-f_\eta, f_\eta]$, sidebands are found centered at kf_o (see $S^{(k)}_{\eta\eta}$ in Fig. 2) and their effects should be combined. Nevertheless, if one is interested in analysing what happens around the generic qf_o harmonic, the $S^{(k)}_{\eta\eta}$ contributions with $k \neq q$ can be ignored provided that they are significantly negligible with respect to $S^{(q)}_{\eta\eta}$.

Several numerical techniques can be found in the literature to obtain the periodic steady state solution of (3) and the spectra of the (small signal) solutions of (5) if Eq. (3) describes the dynamics of a smooth system. In this paper, we resort to an extension toward hybrid dynamic systems of the shooting time-domain analysis to achieve the former [18], [24].[2] As a byproduct of the shooting analysis itself, the time-evolution of the state transition matrix of the circuit, computed along its periodic solution, is available and it is used for the PAC analysis [25].

III. Power System and Power Electronics Circuits Interaction

To illustrate the PAC analysis, this section discusses a particular case study to exemplify how the power system model interacts with a nonlinear power electronics circuit. We will focus on the interconnection between a power system model and a STATCOM device. We assume that the single phase equivalent of the STATCOM symmetric three-phase power-supply circuit is connected to one of the buses of a generic power system model through the $x(t)$ voltage. A steady-state solution of the overall system is assumed to be available and obtained by means of standard techniques, e.g., power flow analysis. In particular, the x_{PF} phasor represents $x(t)$ at the operating point.

A. Equivalent circuit of the nonlinear circuit

Once the x_{PF} phasor is determined, we are interested in modeling the input admittance that relates the variation of the STATCOM current to the variation of the supply voltage. Of course, other transfer functions can be considered, such as, for example, the one that relates the input current and the i_q input reference current.

A PAC analysis of the STATCOM is performed injecting a sequence of tones in the band $[f_o - f_m, f_o + f_M]$ choosing safe values of f_m and f_M such that $f_m < f_\xi$ and $f_M > f_\xi$. This injection range is chosen since the power system interacts with the STATCOM through the $\xi(t)$ signal properly shifted back around $\pm f_o$. In this case, the effects of the injection are evaluated in the same frequency band as the input one, thus neglecting spectrum folding at kf_o for $k \neq 0$. This means that, according to Fig. 2, only the $S^{(0)}_{\eta\eta}$ contribution, whose upper bound is actually greater than f_o being $f_\eta = f_o + f_M$, is considered.

After having obtained the spectrum of the STATCOM frequency response in the $[f_o - f_m, f_o + f_M]$ frequency interval, a linear circuit is build that is able to fit the PAC analysis results in that band.[3] The circuit has to be synthesizable and is then mapped from the power electronics side to the power system one as it is usually done for impedance loads. This model has to be completed to mimic as close as possible the same behaviour of the version of the STATCOM. This aspect is clarified below.

B. PAC equivalent circuit of the power system model

The version of the VSC used to show the application of PAC is that presented in [26]. A detailed description of the circuit and of the linear control loops can be found in [27]. For the sake of clarity, the block schematic of the VSC is shown in Fig. 3. The blocks enclosed by the (red) dashed box constitute the circuit simulated by the shooting analysis followed by the PAC analysis. The VSC is supplied by the $E_{a,b,c}$ star-connected three-phase voltage sources through an input filter (not shown in Fig. 3). The primary controllers of the VSC allow to set the $i_q(t)$ and $i_d(t)$ currents flowing in the three-phase voltage sources. The input of the controller that sets $i_d(t)$ is connected to a Proportional/Integral (PI) block that takes as input the $\mathrm{V_{dc}}$ voltage that is derived from the $\mathrm{V_c}$ DC side voltage as detailed in [26]. The $\mathrm{V_c}$ voltage across the (large) filtering capacitor

[2] In general, this is the only possible solution whenever the circuit is switching or described by an Analog Mixed Signal (AMS) model.

[3] To obtain a more accurate fitting in the $[f_o - f_\xi, f_o + f_\xi]$ frequency interval, i.e., the one in which the power system actually interacts with the STATCOM, it is worth choosing $f_m \ll f_\xi$ and $f_M \gg f_\xi$.

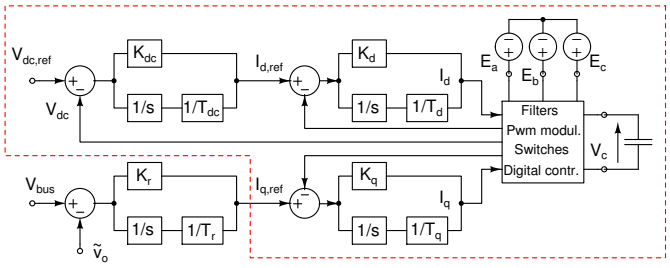

Figure 3. The block schematic of the VSC used as test benchmark. PAC ones.

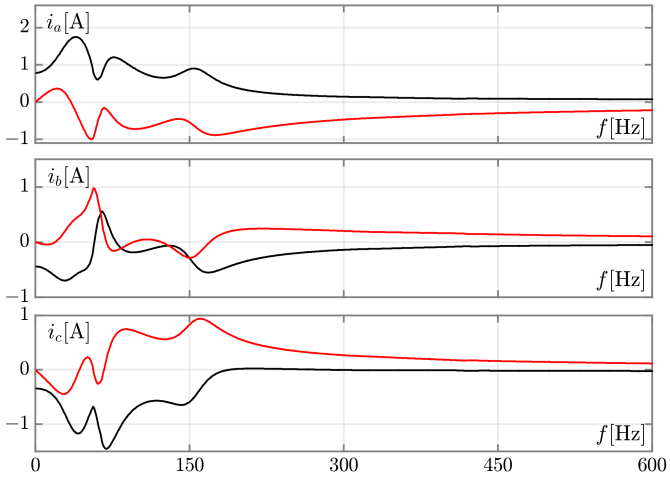

Figure 4. In black and in red the real and imaginary components, respectively, of the VSC small-signal currents across the three-phase independent voltage sources supplying the VSC.

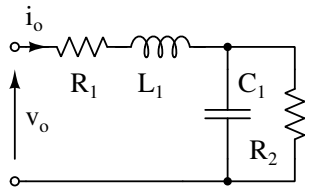

Figure 5. The equivalent dynamic circuit that models the relation between the v_o and i_o branch voltage/current determined by exploiting the PAC analysis. $R_1 = 0.263\,\Omega$, $R_2 = 0.615\,\Omega$, $L_1 = 0.977\,\mathrm{H}$, $C_1 = 23.112\,\mathrm{mF}$.

at the DC side of the VSC is stabilised by the voltage control loop.

The $i_{q,ref}$ is thus the only remaining control input of the STATCOM. In the STATCOM, the $i_{q,ref}(t)$ input is fed by a PI block that takes as input the magnitude of the $\mathrm{V_{bus}}$ three-phase input voltage and control $i_{q,ref}(t)$ to keep such a voltage constant at the $\widetilde{v}_o$ value, as detailed in [26], i.e., another voltage control loop is implemented.

In order to properly design the aforementioned voltage control, it is interesting to study the sensitivity of the $i_q(t)$ input current with respect to the three-phase voltage input sources. This sensitivity is an aggregate indicator of the performance of the controller acting on $i_q(t)$. This is the aspect that we want to model.

In particular, we exploit PAC to derive the model of the input admittance of the STATCOM. The blocks enclosed in the (red) dashed line in the schematic of Fig. 3 are modelled at a detailed level when we apply the PAC analysis. Furthermore, note that the presented modeling flow is of general validity, we apply it to a VSC with the aim to show its effectiveness. In all simulations, we used same parameter values as in [26].

We proceed as follows. We inject a small signal voltage tone that superimposes to the E_a source of the three-phase voltage source and compute the corresponding currents on the a, b and c phases (and hence $i_q(t)$). There is "symmetry" among the injection nodes and the three-phase currents. The f_m and f_M frequency bounds are chosen to have a good fitting of the equivalent lumped network that implements the transfer function computed by the PAC analysis. Experience should suggest the choice of the basic cell and the number of cells that constitutes the lumped network. The parameters of this network are selected to obtain the best fitting that minimises the error between the transfer function by PAC and that of the lumped network.

Fig. 4 shows the transfer functions obtained through the PAC analysis. We then derive the *equivalent single-phase* transfer function and fit the R_1, R_2, C_1 and L_1 parameters of the circuit shown in Fig. 5 to minimise the square error of the real and imaginary components of the transfer function in the $[f_m, f_M]$ bandwidth, i.e., $\Re(i_o(v_o))$ and $\Im(i_o(v_o))$. Finally, the resulting equivalent circuit is redesigned to suit a standard power system model, i.e., the circuit is transformed from a dynamic one to an algebraic one where capacitors and inductors are imaginary impedances. Note that, in this case, the equivalent model has frequency dependent impedances since "instantaneous frequency" of the bus is derived and used to compute the time-varying impedance of the equivalent circuit. We quoted "instantaneous frequency" since its derivation is done after having conditioned the bus voltage as described in [28].

Since the switching sequence of the three phases of the VSC is governed by a phase-locked-loop that synchronises to the power bus instantaneous phase, to model the STATCOM we added a voltage controlled voltage source to the equivalent circuit of Fig. 5 that implements the same feature. In this way, the reactive current injection is synchronous with the phase of the power bus to which the VSC is connected. Finally, based on the circuit shown in Fig. 5, the complete STATCOM model is as follows:

$$i_d = f_d(v_d, v_q) + \frac{\frac{v_d}{n} + \omega(t) L_1 i_{1,q} - v_{c,d} - h_d(v_d, v_q)}{nR_1}$$

$$i_q = f_q(v_d, v_q) + \frac{\frac{v_d}{n} - \omega(t) L_1 i_{1,d} - v_{c,q} - h_q(v_d, v_q)}{nR_1}$$

$$i_{1,d} = \frac{v_{c,d}}{R_2} - \omega(t) C_1 v_{c,q}$$

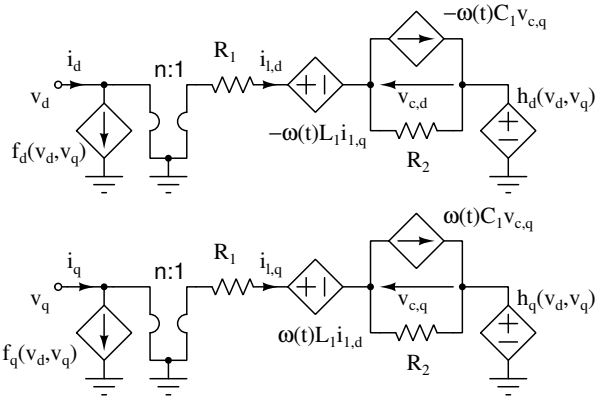

Figure 6. The circuit implementing the proposed model of the STATCOM used in power flow analyses.

$$
\begin{aligned}
i_{1,q} &= \frac{v_{c,q}}{R_2} + \omega(t) C_1 v_{c,d} \qquad (6)\\
h_d(v_d, v_q) &= \widetilde{v}_p v_d(t) \left(v_d^2(t) + v_q^2(t)\right)^{-1/2}\\
h_q(v_d, v_q) &= \widetilde{v}_p v_q(t) \left(v_d^2(t) + v_q^2(t)\right)^{-1/2}\\
T_r \frac{dx}{dt}(t) + x(t) - K_r &\left(\widetilde{v}_o - \sqrt{v_d^2(t) + v_q^2(t)}\right) = 0\\
f_d(v_d, v_q) &= -x(t) v_q(t) + K_p i_{1,d}\\
f_q(v_d, v_q) &= x(t) v_d(t) + K_p i_{1,q}
\end{aligned}
$$

where we have assumed that the VSC is connected to the AC bus by an ideal transformer with tap-ratio n; $\widetilde{v}_p$ is the modulus of the bus voltage computed by the power flow; $\widetilde{v}_o$ is the value of the set-point at which the STATCOM should keep the power bus voltage by regulating the reactive current; K_p is a scaling factor that accounts for the parallel connections of several identical STATCOM; and $\omega(t)$ is the instantaneous frequency of the bus voltage. The first 4 equations in (6) model the input admittance of the VSC. The following 2 equations implement the "phase-locked-loop" and the last 3 equations implement the injection of the active and reactive power (only losses contribute to active power). Note that $i_{1,q} = i_{1,d} = 0$ in the circuit of Fig. 6 at the power flow solution. The complete circuit equivalent model of the VSC, that implements the Eq. (6), is shown in Fig. 6.

IV. Case Study

To test the proposed model, we use the well-known IEEE 14-BUS system, which has been largely used as benchmark system for voltage stability studies as well as for the analysis of the transient response of FACTS devices (see, for example, [29] and [30]). The STATCOM is connected to the BUS14 as suggested in [29]. The system is overloaded by 23% (both loads and generators) and a time domain simulation is performed following the outage at $t = 1$ s of the line connecting BUS02 and BUS04. The bus voltage amplitude at BUS14 is shown in Fig. 7. As expected (see [29]), the bus voltage oscillates and the magnitude of the oscillation increases till stabilizing on a periodic trajectory.

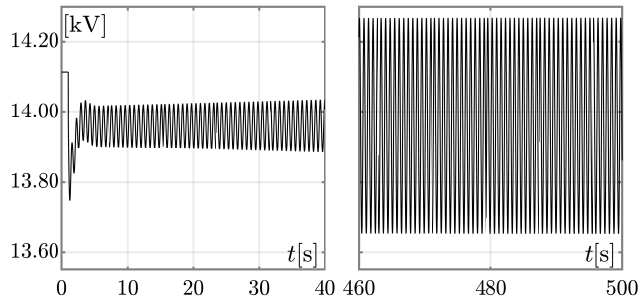

Figure 7. The modulus of the BUS14 voltage obtained with the STATCOM disconnected. In the left panel the initial transient, immediately after the line outage, can be observed. In the right panel the steady state oscillation is shown.

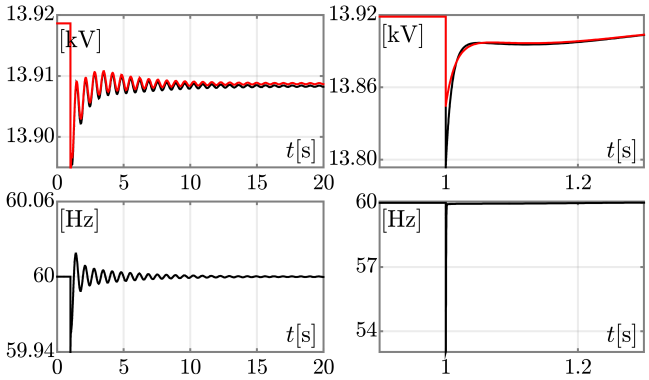

Figure 8. Upper row: the modulus of the BUS14 voltage obtained with the proposed model of the STATCOM (red trace) and with the conventional simple model of the STATCOM (black trace). Lower row: the instantaneous frequency of the bus voltage. The right panels are an enlargement of the left ones around the outage time instant.

The same perturbation was applied using the proposed model of the STATCOM. Results are shown in Fig. 8. We see that modulus of the BUS14 voltage quickly stabilizes (simulation end time is less that the previous one) with limited oscillations. Figure 8 also shows the instantaneous frequency of the bus voltage, estimated with the same approach described in [28]. As it can be seen in Fig. 8, there is a sharp fall to about 53 Hz just at the disconnection of the line. This is due to a sharp variation of the voltage phase since interconnecting lines are modeled through algebraic equations and not through differential ones. Figure 8 also shows the magnitude of the BUS14 voltage when the conventional model of the STATCOM is used. We see that the drop of the bus voltage at the line disconnection is smaller and that the amplitude of the oscillation is reduced with respect to the proposed model. However, it has to be noted that the overall oscillations have a very small relative magnitude in both cases and are almost indistinguishable.

V. Concluding Remarks and Future Work

The paper presents a systematic technique to model nonlinear switched power system devices based on the shooting

method and PAC analysis. Such an approach properly captures the interaction of power system models and highly non linear power electronics circuits, while keeping simple the device models. The proposed approach is general and can be applied, for instance, to the large class of devices based on VSC.

The shooting method and the PAC analysis are typical features of a large number of circuit simulators and this enables deriving the proposed model through standard tools. The main strength of the proposed approach is that the resulting model of the nonlinear (switching) device includes a first order approximation of *all* inherent characteristics of the device itself. On the other hand, a weakness of the models derived through the PAC analysis is that the first order approximation might not be valid for large perturbations. For example, the effect of hard limits cannot be included straightforwardly into the proposed model. However, this issue can be solved by means of defining and interpolating a look-up table that stores the parameters of the equivalent model for different operating conditions and instantaneous frequencies. Future work will focus on this direction.

REFERENCES

[1] C. Zhe, J. M. Guerrero, and F. Blaabjerg, "A Review of the State of the Art of Power Electronics for Wind Turbines," *IEEE Transactions on Power Electronics*, vol. 24, no. 8, pp. 1859–1875, 2009.

[2] T. Ackermann, *Wind Power in Power Systems*. New York: John Wiley & Sons, 2012.

[3] F. Blaabjerg, R. Teodorescu, M. Liserre, and A. V. Timbus, "Overview of Control and Grid Synchronization for Distributed Power Generation Systems," *IEEE Transactions on Industrial Electronics*, vol. 53, no. 5, pp. 1398–1409, 2006.

[4] J. M. C. amd L. G. Franquelo, J. T. Bialasiewicz, E. Galvan, R. Guisado, M. A. M. Prats, J. I. Leon, and N. Moreno-Alfonso, "Power-Electronic Systems for the Grid Integration of Renewable Energy Sources: A Survey," *IEEE Transactions on Industrial Electronics*, vol. 53, no. 4, pp. 1002–1016, 2006.

[5] T. Petersson and K. Frank, "Starting of Large Synchronous Motor using Static Frequency Converter," *IEEE Transactions on Power Apparatus and Systems*, vol. PAS-91, no. 1, pp. 172–179, 1972.

[6] G. Magsaysay, T. Schuette, and R. J. Fostiak, "Use of a Static Frequency Converter for Rapid Load Response in Pumped-Storage Plants," *IEEE Transactions on Energy Conversion*, vol. 10, no. 4, pp. 694–699, 1995.

[7] A. Yazdani and R. Iravani, *Voltage-Sourced Converters in Power Systems. Modeling, Control and Applications*, 1st ed. Wiley-IEEE Press, 2010.

[8] S. Cole, "Steady-State and Dynamic Modelling of VSC HVDC Systems for Power System Simulation," Ph.D. dissertation, Katholieke Universiteit Leuven, Sep. 2010.

[9] N. R. Chaudhuri, R. Majumder, B. Chauduri, and J. Pan, "Stability Analysis of VSC MTDC Grids Connected to Multimachine AC Systems," *IEEE Transactions on Power Delivery*, vol. 26, no. 4, pp. 2774–2784, Oct. 2011.

[10] E. Acha and B. Kazemtabrizi, "A New STATCOM Model for Power Flows Using the NewtonRaphson Method," *IEEE Transactions on Power Systems*, vol. 28, no. 3, pp. 2455–2465, Aug. 2013.

[11] N. R. Chaudhuri, B. Chauduri, R. Majumder, and A. Yazdani, *Multi-terminal Direct-current Grids: Modeling, Analysis, and Control*. John Wiley & Sons, 2014.

[12] J. Beerten, S. Cole, and R. Belmans, "Modeling of Multi-Terminal VSC HVDC Systems With Distributed DC Voltage Control," *IEEE Transactions on Power Systems*, vol. 29, no. 1, pp. 34–42, Jan. 2014.

[13] D. Xia and G. Heydt, "Harmonic Power Flow Studies Part I - Formulation and Solution," *IEEE Trans. Power App. Syst.*, vol. PAS-101, no. 6, pp. 1257–1265, Jun. 1982.

[14] ——, "Harmonic Power Flow Studies - Part II Implementation and Practical Application," *IEEE Trans. Power App. Syst.*, vol. PAS-101, no. 6, pp. 1266–1270, Jun. 1982.

[15] T. Demiray, F. Milano, and G. Andersson, "Dynamic phasor modeling of the doubly-fed induction generator under unbalanced conditions," in *IEEE Power Tech*. IEEE, 2007, pp. 1049–1054.

[16] M. Nakhla and J. Vlach, "A piecewise harmonic balance technique for determination of periodic response of nonlinear systems," *Circuits and Systems, IEEE Transactions on*, vol. 23, no. 2, pp. 85–91, Feb 1976.

[17] Y. Sun, G. Zhang, W. Xu, and J. Mayordomo, "A Harmonically Coupled Admittance Matrix Model for AC/DC Converters," *IEEE Trans. Power Syst.*, vol. 22, no. 4, pp. 1574–1582, Nov. 2007.

[18] F. Bizzarri, A. Brambilla, and G. Storti Gajani, "Extension of the variational equation to analog/digital circuits: numerical and experimental validation," *International Journal of Circuit Theory and Applications*, vol. 41, no. 7, pp. 743–752, 2013.

[19] F. Bizzarri, A. Brambilla, and S. Saggini, "Voltage regulators design through advanced mixed-mode circuit simulation," *IEEE Trans. Power Electron.*, vol. 29, no. 9, pp. 4496–4499, 2014.

[20] R. Telichevesky, K. Kundert, and J. White, "Efficient AC and noise analysis of two-tone RF circuits," in *33rd Design Automation Conference Proceedings*, Jun. 1996, pp. 292–297.

[21] D. Kuznetsov and J. Schutt-Aine, "Optimal transient simulation of transmission lines," *IEEE Trans. Circuits Syst. I*, vol. 43, no. 2, pp. 110–121, Feb. 1996.

[22] V. Venkatasubramanian, "Tools for dynamic analysis of the general large power system using time-varying phasors," *International Journal of Electrical Power & Energy Systems*, vol. 16, no. 6, pp. 365–376, 1994.

[23] E. J. W. ter Maten, J. G. Fijnvandraat, C. Lin, and J. M. F. Peters, "Periodic ac and periodic noise in rf simulation for electronic circuit design," in *Modeling, Simulation, and Optimization of Integrated Circuits*, ser. ISNM International Series of Numerical Mathematics, K. Antreich, R. Bulirsch, A. Gilg, and P. Rentrop, Eds. Birkhuser Basel, 2003, vol. 146, pp. 121–134.

[24] F. Bizzarri, A. Brambilla, and G. Storti Gajani, "Steady State Computation and Noise Analysis of Analog Mixed Signal Circuits," *IEEE Trans. Circuits Syst. I*, vol. 59, no. 3, pp. 541–554, Mar. 2012.

[25] F. Bizzarri, A. Brambilla, and G. Storti Gajani, "Periodic small signal analysis of a wide class of type-II phase locked loops through an exhaustive variational model," *Circuits and Systems I: Regular Papers, IEEE Transactions on*, vol. 59, pp. 2221–2231, 2012.

[26] C. Sao, P. Lehn, M. Iravani, and J. Martinez, "A benchmark system for digital time-domain simulation of a pulse-width-modulated d-statcom," *Power Delivery, IEEE Transactions on*, vol. 17, no. 4, pp. 1113–1120, Oct 2002.

[27] K. L. Lian and M. Syai'in, "Steady-state solution of a voltage source converter with dq-frame controllers by means of the time-domain mathod," *Electrical and Electronic Engineering, IEEJ Transaction on*, vol. Published online in Wiley Online Library, DOI: 10.1002/tee.21952, 2014.

[28] F. Milano, L. Vanfretti, and J. C. Morataya, "An open source power system virtual laboratory: The psat case and experience," *Education, IEEE Transactions on*, vol. 51, no. 1, pp. 17–23, Feb 2008.

[29] C. A. Cañizares and Z. T. Faur, "Analysis of svc and tcsc controllers in voltage collapse," *Power Systems, IEEE Transactions on*, vol. 14, no. 1, pp. 158–165, Feb 1999.

[30] F. Milano, *Power System Modelling and Scripting*. London: Springer, 2010.